Physics Letters A 383 (2019) 125778

Contents lists available at ScienceDirect

Physics Letters A

www.elsevier.com/locate/pla

Temperature-dependent XAFS study of the local lattice distortion of the CuO_2 plane in $Sr_2CuO_{3+\delta}$ powder sample

Haibo Wang [a], Ying Liu [c], Zhenlin Luo [b], Qingqing Liu [c], Yuanjun Yang [b], Haoliang Huang [b], Mengmeng Yang [b], Changqing Jin [c,*], Chen Gao [b,d,*]

[a] Editorial Department, Tonghua Normal University, Tonghua, Jilin 134002, China
[b] National Synchrotron Radiation Laboratory, University of Science and Technology of China, Hefei, Anhui 230026, China
[c] Institute of Physics, Chinese Academy of Sciences, Beijing 100080, China
[d] CAS Key Laboratory of Materials for Energy Conversion and Collaborative Innovation Center of Chemistry for Energy Materials, University of Science and Technology of China, Hefei, Anhui 230026, China

ARTICLE INFO

Article history:
Received 21 March 2019
Received in revised form 10 June 2019
Accepted 11 June 2019
Available online 9 July 2019
Communicated by L. Ghivelder

Keywords:
XAFS
Local lattice distortion
Superconductivity
$Sr_2CuO_{3+\delta}$

ABSTRACT

In order to study the relationship between local lattice distortion and superconductivity, we performed temperature dependent x-ray absorption fine structure (XAFS) on $Sr_2CuO_{3+\delta}$ powder sample (single phase with $T_c = 48$ K). The temperature dependent Debye-Waller factor of Cu-O pair appears an anomalous upturn at 90 K and becomes drop around the superconducting transition temperature of ~50 K. It means that local lattice distortion appears at 90 K. Furthermore, the analysis of temperature dependent X ray Absorption Near Edge Structure (XANES) shows that the R factor, which denotes the inhomogeneous charge density distribution, shows a sharp drop at 90 K. According to previous reports on other doped 214 cuprates, the above experimental results reveal that the local lattice distortion at Cu site in CuO_2 plane occurs with the inhomogeneous charge density distribution at 90 K. It indicates that the inhomogeneous charge density distribution may be caused by the local lattice distortion at Cu site before superconductive order formation, implying that electron-lattice interaction play a key role in superconductivity of $Sr_2CuO_{3+\delta}$.

1. Introduction

In recent, perovskite-layered high temperature cuprate superconductors, whose CuO_2 conducting layer are sandwiched by two rock-salt layers, are studied extensively [1–8]. The intact and symmetric CuO_2 plane is approved for improving high temperature superconductivity. In the past few years, many investigations showed that the inhomogeneous charge density distribution coming from the interplay of charge and spindegrees of freedom in the CuO_2 plane may affect high temperature superconductivity [9–14]. Due to the appearance of d-wave superconductive order, the smaller isotope effect on T_c and antiferro magnetic properties of the undoped insulating parent cuprates, the lattice distortion was usually ignored or seen as the unimportant factor for charge transport. However, recent studies, i.e. local lattice distortion and s-wave superconductive order, indicate that the lattice degree of freedom also plays an important role in the formation of high temperature superconductivity of cuprates [15–18]. So, electron-phonon model or electron-polaron model were mentioned for interpreting high temperature superconductivity of cuprates. Therefore, the local lattice distortion becomes one of the most important features of doped cuprates superconductors. $La_{1.48}Sr_{0.12}Nd_{0.4}CuO_4$ is a typical superconducting material with charge density wave below 60 K [15,16,19]. At the same time, a hint of information about the local lattice distortion in the CuO_2 plane is received from the anomalous change of Debye-Waller factor of Cu-O pair at 60 K. The temperature-dependent evolution of XANES spectra weight, which indicates the charge density redistribution, also shows a clear anomalous characteristic below 60 K. The intimate relationship between local lattice effect and electron feature implies that electron-lattice interaction may play a key role in interpreting the superconductivity mechanism of $La_{1.48}Sr_{0.12}Nd_{0.4}CuO_4$. Similar conclusion can be found in the temperature-dependent XAFS studies of $La_{1.875}Ba_{0.125}CuO_4$ and $La_{1.94}Sr_{0.06}CuO_4$ [17–19]. Above all experimental results demonstrate that studying the local lattice effect is significant for understanding high T_c superconductivity of cuprates. Therefore, it is necessary to further study the relationship between local lattice effect and superconductivity in cuprates.

* Corresponding authors.
E-mail addresses: zlluo@ustc.edu.cn (Z. Luo), cgao@ustc.edu.cn (C. Gao).

https://doi.org/10.1016/j.physleta.2019.06.016
0375-9601/

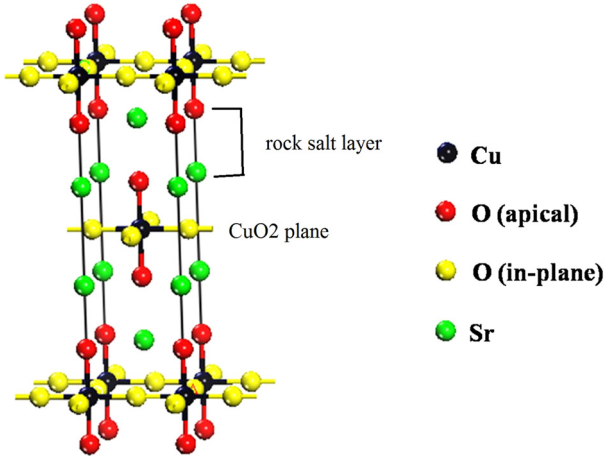

Fig. 1. Schematic crystal structure of $Sr_2CuO_{3+\delta}$ with tetragonal unit cell.

$Sr_2CuO_{3+\delta}$ is a typical 214-type cuprate superconductor. The crytal structure of $Sr_2CuO_{3+\delta}$ is shown in Fig. 1. It belongs to the I4/mmm space group. When delta equals 0.4, it reaches the optimal doping state. At this time, its crystal lattice is Changshu a=b=0.3795 nm, c=1.2507 nm. Its cell belongs to perovskite structure. As the center of perovskite structure, the oxygen atom is closest to the copper atom (absorption atom), so it corresponds to the first peak in FT spectrum. As the apex of perovskite structure, strontium atom is next to copper atom (absorption atom), so it corresponds to the second peak in FT spectrum. On the CuO_2 plane, the copper atom sharing one oxygen atom with the absorption copper atom naturally becomes the third nearest neighbor atom. Its T_c is much higher than others [20–22]. Previous studies show that the superstructure observed at room temperature is related with the much higher T_c value of $Sr_2CuO_{3+\delta}$ [22–25]. The superstructure of $Sr_2CuO_{3+\delta}$ was considered to be the result of the displacement of Sr atoms or the oxygen vacancies modulated structure. Hiroi et al. firstly synthesized this material and reported a superstructure with unit-cell parameters $4\sqrt{2}a_p \times 4\sqrt{2}a_p \times c_p$ [21]. Then, Adachi [23] and Wang et al. [24] found a Fmmm superstructure with unit-cell parameters $5\sqrt{2}a_p \times 5\sqrt{2}a_p \times c_p$. After few years, the majority Fmmm and minority C2/m superstructures were observed simultaneously in as-prepared sample ($T_c = 75$ K) at room temperature by Liu et al. [25]. These superstructures were all considered related with superconductivity of $Sr_2CuO_{3+\delta}$ material. However, the origin of these superstructures is unclear now. Shimakawa et al. reported that the superstructure was originated from Sr atoms displacement [26]. Liu et al. indicated that the oxygen vacancies ordering was the reason for forming these superstructures [25]. Whether the behavior of Sr atoms or oxygen vacancies, they are nearby the Cu atoms in CuO_2 plane. So, studying the local lattice structure at Cu site of CuO_2 plane is very important for understanding the superconductivity in this material.

X-ray Absorption Fine Structure (XAFS) spectra is extensively used for studying the local structure of crystal materials. Extended X-ray Absorption Fine Structure (EXAFS), which can provide instantaneous local structure information, is a powerful tool for studying the local lattice distortion. At the same time, the Cu K-edge X-ray absorption near edge structure (XANES) is the result of multiple scattering of photoelectrons emitted at the Cu site. Therefore, XANES can give the electron distribution information around CuO_2 plane. In addition, with the development of synchrotron radiation, the temperature dependent XAFS technique becomes more effective for characterizing the weak signal coming from local structure evolution [27–32]. Here, we perform temperature-dependent Cu K-edge XAFS on $Sr_2CuO_{3+\delta}$ powder sample ($T_c \sim 48$ K) to reveal the relationship between local lattice distortion and superconductivity of this material. Details are described as follows.

2. Experiments and calculations

Temperature-dependent Cu K-edge XAFS study of $Sr_2CuO_{3+\delta}$ powder sample was performed at the beamline 1W1B of Beijing Synchrotron Radiation Facility. The synchrotron light was introduced to 1W1B from a seven-period wiggler placed in the storage ring. The $Sr_2CuO_{3+\delta}$ powder sample was synthesized under high temperature and high pressure. The detail synthesis condition was described in reference [33]. T_c is about 48 K. And the nominal value of δ is about 0.4. All measurements were performed in transmission mode. In order to make the edge jump around absorption edge is close to 1, the powder sample was mixed with graphite and pressed into tablets for achieving transmission experiment. The tablet sample was mounted on a copper sample holder in the closed cycle He cryostat for lowing the temperature on sample. The measurement was conducted at six temperature points with an accuracy of ± 2 K. At the same time, ionization chambers were used for recording x-ray counts of incoming light and transmission light. Enough counting time at each data point is necessary for better signal to noise ratio of XAFS. Standard procedure was used for extracting EXAFS signal, coordination information and Debye-Waller factor [34]. The phase corrected EXAFS was fitted by non-linear least squares fitting using the curved wave theory. The effective coordination number was kept constant while the radial distance and the correlate thermal fluctuations given by the Debye-Waller factor ($\sigma 2$) for the Cu-O (planar) were allowed to vary. Individual EXAFS data (k<15 Å-1) for neighbor correlations are filtered and curve fitted in k-space using a single scattering formula with theoretical phase shift functions calculated by FEFF6. The fitting procedure is based on a standard nonlinear least square technique which minimizes the statistical χ^2 determined by the squares of the difference between experimental and theoretical fitting data. The errors in the parameters were estimated by the standard EXAFS (parabola) method in which the quality of fit parameter (proportional to the statistical χ^2) is plotted as a function of the concerned parameter. Errors are usually estimated from a fractional increase d of χ^2 above its minimum value.

Based on Multiple Scattering Theory, the theoretical calculation for XANES at different temperature was carried out by FDMNES program [35]. It was performed for reproducing the Cu K-edge XANES of $Sr_2CuO_{3+\delta}$ powder sample. The $Sr_2CuO_{3+\delta}$ crystal structure cluster model is established for this calculation. The cluster radius is 6.0 Å. All of possible scattering paths between absorbing atom and coordination atoms were discussed in this calculation. And electric dipole and electric quadrupole components contributing to electron transition at Cu K-edge were considered for reproducing XANES. Fermi energy was about -3.5 eV.

3. Results and discussion

3.1. Temperature dependence of FT magnitude function of $Sr_2CuO_{3+\delta}$

To study the temperature dependence of local lattice structure at Cu site in CuO_2 plane, the normalized XAFS spectra and the Fourier transform (FT) magnitude function (multiplied by k^3) of $Sr_2CuO_{3+\delta}$ powder sample at different temperatures are firstly measured and plotted in Fig. 2 and Fig. 3. The position of these peaks at XANES was similar, but the intensity had smaller difference. However, the position and the shape of these peaks at EXAFS part were different. In order to detect the difference, the Fourier transform (FT) magnitude function (multiplied by k^3) was done. In Fig. 3, the positions of these peaks are not corrected for the photoelectron back-scattering phase shifts, so the peak positions do not

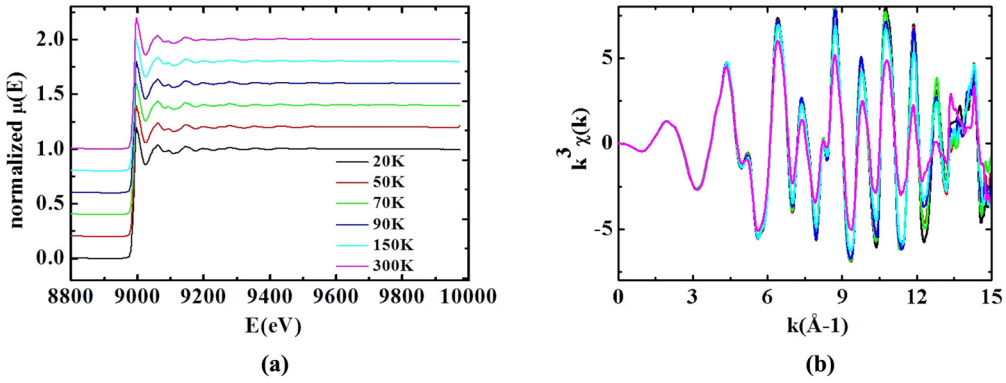

Fig. 2. Different temperatures of $Sr_2CuO_{3+\delta}$ samples: (a) normalized XAFS full spectrum of Cu K absorption edge; (b) k-space EXAFS oscillation function.

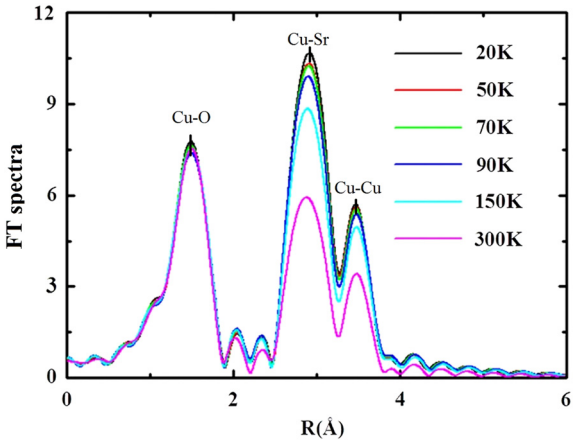

Fig. 3. Temperature dependence of Fourier transform magnitude function (multiplied by k^3) of $Sr_2CuO_{3+\delta}$.

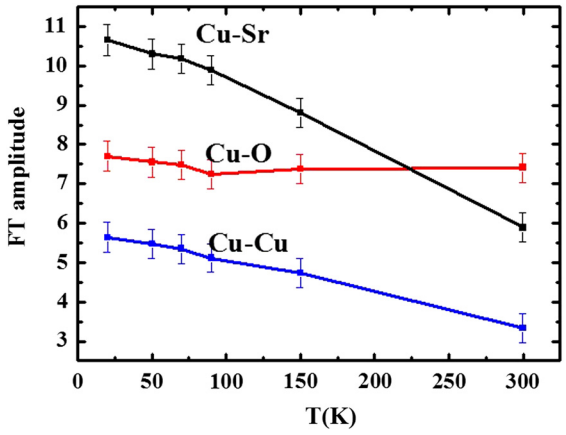

Fig. 4. Temperature dependence of the amplitudes of the main peaks in the Fourier transforms shown in Fig. 2.

denote the real bond length. Three strong peaks in Fourier transform spectra are respectively corresponding to Cu-O, Cu-Sr and Cu-Cu (sharing the same oxygen atom with absorbing atom Cu) pairs, which is illustrated by the crystal structure of $Sr_2CuO_{3+\delta}$. The peak positions have no change with the lowing temperature, however the intensity of these peaks change clearly. In addition, in the powder sample, the bond length of Cu-O planar and Cu-O apical is very close. However, the coordination number of oxygen in-plane for Cu is larger than the apical oxygen. At the same time, the oxygen vacancies were considered occupying at apical sites. The contribution of Cu-O apical is small. So the Cu-O mainly refers to the Cu-O planar.

Fig. 4 represents the temperature dependence of FT amplitude for Cu-O, Cu-Sr and Cu-Cu pairs. When the temperature decreases from 300 K to 20 K, the FT amplitude of Cu-Sr next nearest neighbor coordination and Cu-Cu third nearest neighbor coordination both increase obviously [15]. However, the variation of FT amplitude of Cu-O nearest neighbor coordination is not obvious comparing with the Cu-Sr and Cu-Cu pairs in the whole temperature region. The difference may due to the different coupling level. The stronger coupling interaction between Cu and O atom in CuO_2 plane make the Cu-O coordination is not easily disturbed with external factors. However, the other coordination atoms are far from the Cu atoms, the smaller coupling interaction make Cu-Sr next nearest neighbor coordination and Cu-Cu third nearest neighbor coordination easily change with temperature.

3.2. Temperature dependence of Debye-Waller factors

For further study, we pay attention to the temperature-dependent Debye-Waller factor of Cu-O, Cu-Sr and Cu-Cu pairs. The Debye-Waller factor is a good indicator of local lattice distortion. Both the static and dynamic local lattice distortions are all taken into account in the temperature dependent Debye-Waller factors. The Fourier transform magnitude function of Cu-Sr, Cu-Cu pairs are fitted simultaneously for getting the Debye-Waller factor corresponding to each coordination shell. The fitting results are shown in Fig. 5. The fitting range was selected from 1 Å to 4 Å. The fitting results shows well in this range. In order to study the Debye-Waller factor of Cu-O pair, due to the small change of the intensity of Cu-O peak, the Cu-O peak is separated by Hanning window, and its EXAFS oscillation function is obtained by inverse Fourier transform. The fitting result is shown in Fig. 6. According to the fitting, the coordination number for Cu-O, Cu-Sr, Cu-Cu were set as 6, 8, 4. In meantime, the coordination distance for Cu-O, Cu-Sr, Cu-Cu were 1.898 Å, 2.912 Å, 3.795 Å. According to the fitting, the temperature-dependent Debye-Waller factors of Cu-O, Cu-Sr and Cu-Cu pairs are extracted from the fitting parameters and presented in Fig. 7. In Fig. 7 (a), the temperature dependence of Debye-Waller factors of the Cu-Sr and Cu-Cu pairs behave like the correlated Debye model. The feature of $\sigma^2_{Cu-Sr} - T$ and $\sigma^2_{Cu-Cu} - T$ is similar. The Debye-Waller factors of the Cu-Sr and Cu-Cu pairs all increases with the lowing temperature. Particularly, it increases in a large magnitude when the temperature is above T_c, which is reasonable from the viewpoint of thermal expansion. The smaller variation of the Debye-Waller factor in lower temperature suggests the small strain between rock-salt layer and CuO_2 plane favoring more conductive in superconducting state.

Specially, please note the temperature dependence of Debye-Waller factor of the Cu-O pair around Cu site of CuO_2 plane, which is always largely related with superconductivity of cuprates. So the Debye-Waller factor of the Cu-O pairs is mainly discussed. The

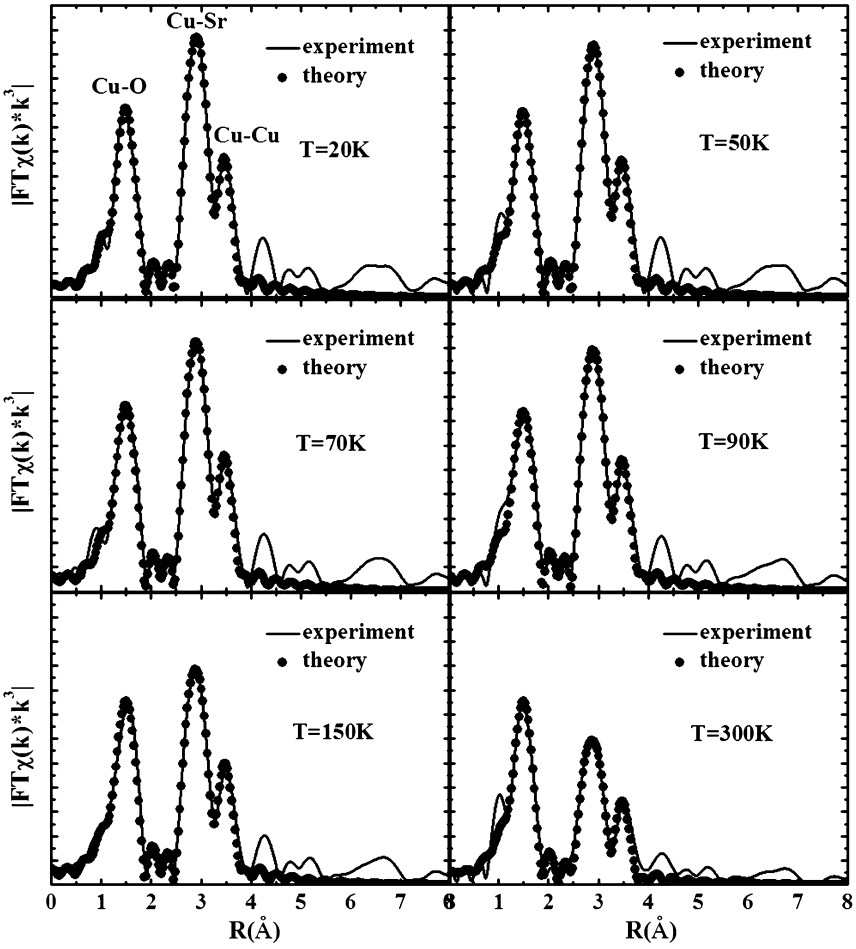

Fig. 5. Fittings and experimental results of Fourier transform magnitude function at different temperatures.

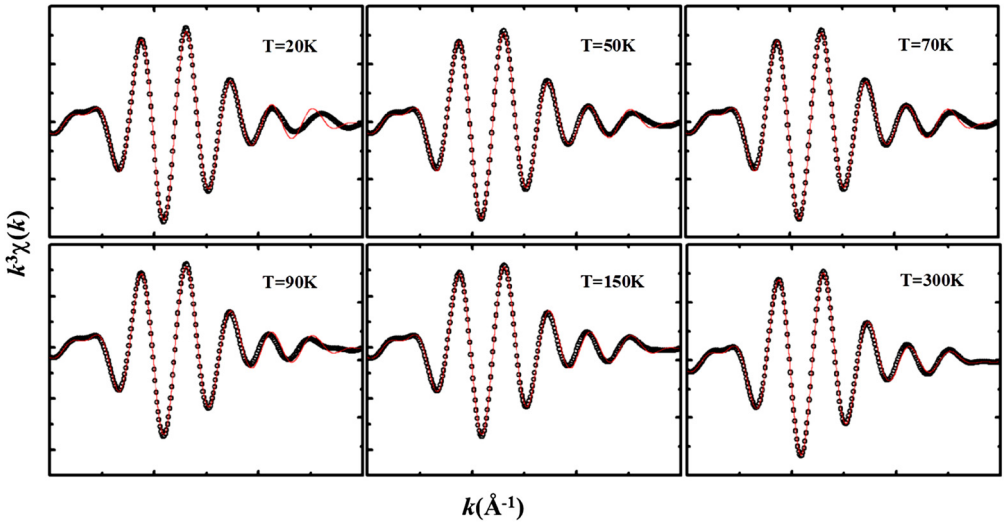

Fig. 6. EXAFS oscillation function and fitting of $Sr_2CuO_{3+\delta}$ superconducting sample ($T_c = 48$ K) with different temperature of Cu-O coordination.

temperature dependence of Debye-Waller factor of Cu-O pair is depicted in Fig. 7 (b). The temperature evolution behavior deviates from correlated Debye model. Anomalous characteristic is observed at low temperature. A kink comes up when the temperature decreases to around T_c. The temperature dependent Debye-Waller factor of Cu-O pairs becomes to rise at ∼90 K, and when the temperature comes to 50 K, the value reaches maximum and becomes drops rapidly. These facts show that the temperature dependence of σ^2_{Cu-O} is completely different from the features of $\sigma^2_{Cu-Sr} - T$ and $\sigma^2_{Cu-Cu} - T$. Similar features are also found in the LNSCO, LSCO, LBCO cuprates [17–19]. The anomalous characteristics of $\sigma^2_{Cu-O} - T$ indicate the arising of local lattice distortion in the CuO_2 plane. In $Sr_2CuO_{3+\delta}$ with $T_c = 48$ K, the local lattice distortion appears at ∼90 K. This conclusion is similar with other doped cuprates superconductors [17–19].

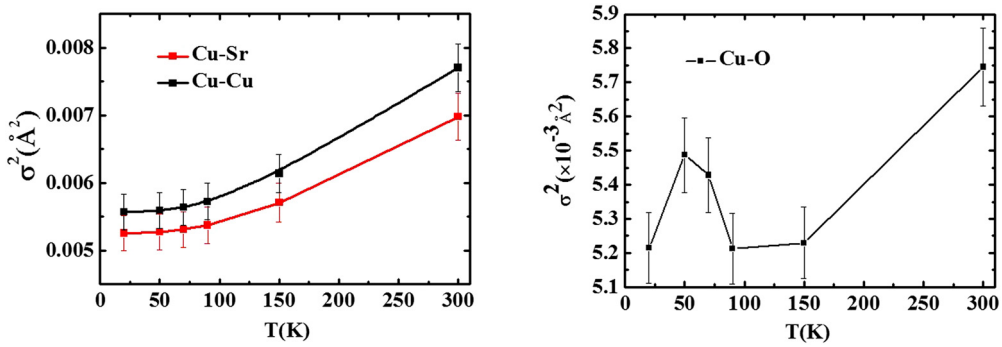

Fig. 7. Temperature dependence of the correlated Debye-Waller factors of (a) the Cu-Sr (σ^2_{Cu-Sr}) pair and Cu-Cu (σ^2_{Cu-Cu}) pair and (b) Cu-O (σ^2_{Cu-O}) pair.

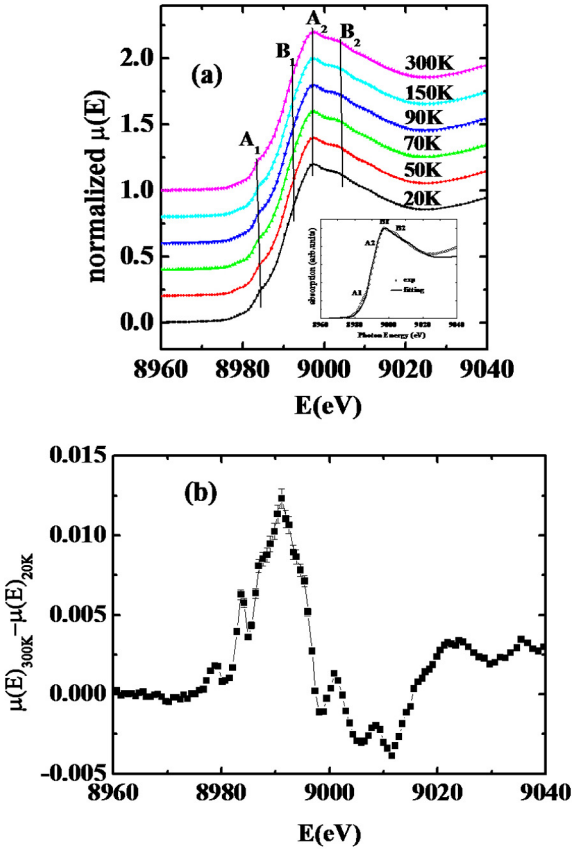

Fig. 8. (a) Temperature dependence of Cu K-edge XANES of the $Sr_2CuO_{3+\delta}$. The inset is the fitting (circle) and experimental result (solid line) for Cu K-edge XANES at 20 K. (b) Difference spectrum between 300 K and 20 K.

3.3. *Temperature dependence of XANES of* $Sr_2CuO_{3+\delta}$

In order to further study the possible charge density redistribution related with local lattice distortion at Cu site, the temperature-dependent XANES spectra of $Sr_2CuO_{3+\delta}$ were studied. At the same time, the multiple scattering calculations were made for interpreting the electron behavior correlated to XANES. In this calculation, the Q_2-distorted CuO_6 octahedron is used for this calculation [15]. The result is shown in Fig. 8 (a). The inset of Fig. 8 (a) show the temperature-dependent XANES spectra of $Sr_2CuO_{3+\delta}$. The fitting results shows well in the range of near edge due to the fitting range from 8960 eV to 9020 eV. The deviation during 9020 eV to 9040 eV may due to the contribution of EXAFS. There are four main peaks A_1, A_2, B_1, B_2 in XANES. The peaks denoted by A_1 and A_2 are due to the photoelectrons ejection from apical oxygen and Sr atoms in rock-salt layer while the peak B_1 is related with multiple scattering of photoelectron between oxygen and copper in CuO_2 plane. The peak B_2 is the contribution of many body effect. In order to distinguish the difference of charge density distribution around T_c, the difference of XANES spectra between 300 K and 20 K are plotted in Fig. 8 (b) to present the amplitude differences of these absorption peaks. The spectra weight transfer occurs with the maximal difference of 1.2% of the normalized intensity. It indicates that the charge density redistribution may happen at Cu site of the CuO_2 plane when the temperature decreases from 300 K to 20 K.

For discussing charge density feature around absorbing atom, the temperature dependence of R factor of $Sr_2CuO_{3+\delta}$ is calculated and shown in Fig. 9, where $R=(b_1-a_1)/(b_1+a_1)$, a_1 is the intensity of peak A_1, b_1 the intensity of peak B_1, the A1 and A2 features are due to the 1s-4p*(π) transition, while B1 and B2 are assigned to the 1s-4p*(σ) transition. A_1 and B_1 stand for the core level excitation of Cu $1s\rightarrow 4p_z$ and Cu $1s\rightarrow 4p_{x,y}$. According to the direction of charge transfer in high temperature cuprate superconductors,

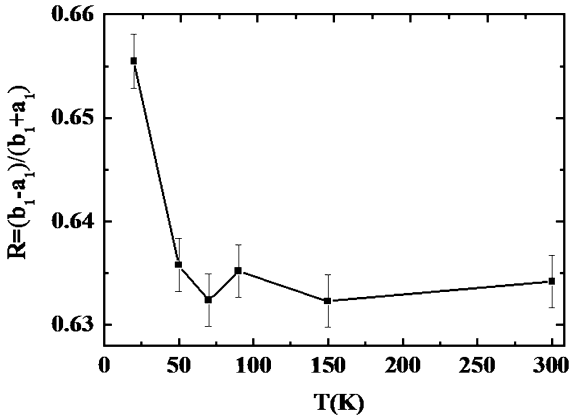

Fig. 9. Temperature evolution of the peak intensity ratio $R=(b_1-a_1)/(b_1+a_1)$ for the $Sr_2CuO_{3+\delta}$ powder. The ratio shows a clear change across the 90 K.

the temperature dependence of R factor should show an increasing tendency with decreasing temperature. However, the value of R has a sudden decrease starting from 90 K, indicating the charge density redistribution at Cu site. At the same time, this transition point is consistent with the starting point of local lattice distortion. It demonstrates that local lattice distortion and charge density redistribution formed beginning from 90 K.

3.4. The relationship between local lattice distortion and superconductivity

The above experiments show that both local lattice distortion and inhomogeneous charge density distribution in CuO_2 plane all happens from 90 K. Although there is only one point at 90 K, the similar deed can be found in other 214 cuprate superconductors [15–18]. According to previous XAFS studies and local structure ordering results of other 214 cuprate superconductors [15–18], the anomalous deed at 90 K may due to the local lattice distortion. The local lattice distortion may indicate the formation of some ordering structure and further make the charge density around Cu atoms redistribute. Therefore, we conclude that the low-temperature ordering structure is correlated with lattice effect. When the temperature further decreases to about 50 K, there is a kink. When the temperature lower than 50 K, the Debye-Waller factor of Cu-O pair becomes to drop, the superconducting order may form. Superconductive coherence makes the material appear superconductivity. According to above all analysis, the lattice effect may provide the medium for electron pairs in superconductive state. In other words, the electron-lattice interaction may be vital in interpreting superconductivity in this kind of layered cuprates.

4. Conclusion

In summary, we reported local lattice distortion and charge density redistribution around Cu site in the CuO_2 plane of $Sr_2CuO_{3+\delta}$ powder through the temperature-dependent XAFS at Cu K-edge. The anomalous characteristic of $\sigma^2_{Cu-O} - T$ implies the local lattice distortion occurring in CuO_2 plane at 90 K. The temperature dependence of R factor, which indicates charge density redistribution, also shows the abnormal feature as similar as $\sigma^2_{Cu-O} - T$. The coexistence of the local lattice distortion and charge density redistribution at Cu site of CuO_2 plane indicates that electron-lattice interaction remains important for interpreting superconductivity in this kind of layered superconductor.

Acknowledgements

The work was supported by the National Basic Research Program of China (973 Program) (2012CB922004/3, 2010CB934501, 2009CB929502), the Science and technology topics of Jilin Provincial Department of Education in 13th Five-Year (JJKH20180860KJ) and the Natural Science Foundation of China (WK2310000043). The authors appreciate the beam time from BL1W1B of Beijing Synchrotron Radiation Facility.

References

[1] W. Zhang, T. Miller, C.L. Smallwood, et al., Sci. Rep. 6 (2016) 29100.
[2] T. Morinari, Relationship between pseudogap temperature and short-range antiferromagnetic order in high-temperature cuprate superconductor, J. Phys. Soc. Jpn. (2018).
[3] D. Rybicki, M. Jurkutat, S. Reichardt, et al., Nat. Commun. 7 (2016) 11413.
[4] N. Poccia, A. Ricci, G. Campi, et al., Supercond. Sci. Technol. 30 (3) (2017).
[5] P. Peczkowski, M. Kowalik, P. Zachariasz, et al., Phys. Status Solidi (2018) 1700888.
[6] X. Sun, W.T. Zhang, L. Zhao, et al., 中国物理快报：英文版 35 (1) (2018) 98–102.
[7] Xuan, Zhang, WenTao, et al., 中国物理快报：英文版 35 (1) (2018) 98–102.
[8] A. Sugimoto, T. Ekino, A.M. Gabovich, et al., Phys. Rev. B 95 (17) (2017).
[9] A. Baum, Y. Li, M. Tomić, et al., Arxiv.Org, 2018.
[10] Jeongseop A. Lee, Y. Xin, et al., New J. Phys. 19 (3) (2017).
[11] D. Agterberg, A. Amin, Interplay of pair density wave and charge density wave order in the cuprate pseudogap phase, in: APS Meeting, APS Meeting Abstracts, 2016.
[12] P.G. Baity, G. Saraswat, Dragana Popović, et al., Avalanches and hysteresis at the structural transition in stripe-ordered $La_{1.48}Nd_{0.4}Sr_{0.12}CuO_4$, in: APS Meeting, APS Meeting Abstracts, 2016.
[13] J. Chang, E. Blackburn, O. Ivashko, et al., Nat. Commun. 7 (2016) 11494.
[14] D. Pelc, M. Vučković, H.J. Grafe, et al., Nat. Commun. 7 (2016) 12775.
[15] N. Ichikawa, S. Uchida, J.M. Tranquada, T. Niemoller, P.M. Gehring, S.H. Lee, J.R. Schneider, Phys. Rev. Lett. 85 (8) (2000) 1738–1741.
[16] J.M. Tranquada, N. Ichikawa, S. Uchida, Phys. Rev. B 59 (22) (1999) 14712–14722.
[17] A. Lanzara, N.L. Saini, T. Rossetti, A. Bianconi, H. Oyanagi, H. Yamaguchi, Y. Maeno, Solid State Commun. 97 (2) (1996) 93–96.
[18] H. Oyanagi, C.J. Zhang, A. Tsukada, M. Naito, J. Supercond. Magn. 22 (2) (2009) 165–168.
[19] N.L. Saini, H. Oyanagi, Z.Y. Wu, A. Bianconi, J. Supercond. Sci. Technol. 15 (3) (2002) 439–445.
[20] Q.Q. Liu, H. Yang, X.M. Qin, Y. Yu, L.X. Yang, F.Y. Li, R.C. Yu, C.Q. Jin, S. Uchida, Phys. Rev. B 74 (10) (2006) 100506.
[21] Z. Hiroi, M. Takano, M. Azuma, Y. Takeda, Nature 364 (6435) (1993) 315–317.
[22] P.D. Han, L. Chang, D.A. Payne, Physica C 228 (1) (1994) 129–136.
[23] S. Adachi, H. Yamauchi, S. Tanaka, N. Môri, Physica C, Supercond. 212 (1) (1993) 164–168.
[24] Y.Y. Wang, H. Zhang, V.P. Dravid, L.D. Marks, P.D. Han, D.A. Payne, Physica C, Supercond. 255 (3) (1995) 247–256.
[25] H. Yang, Q.Q. Liu, F.Y. Li, C.Q. Jin, R.C. Yu, Supercond. Sci. Technol. 20 (10) (2007) 904–910.
[26] Y. Shimakawa, J.D. Jorgensen, J.F. Mitchell, et al., Physica C, Supercond. 228 (1) (1994) 73–80.
[27] D.C. Koningsberger, B.L. Mojet, G.E. Van Dorssen, D.E. Ramaker, Top. Catal. 10 (3–4) (2000) 143–155.
[28] A. Saha, S. Chattopadhyay, T. Shibata, et al., J. Phys. Chem. C 120 (33) (2016).
[29] J. Huang, Q. Liu, T. Yao, et al., XAFS study on structure-activity correlations of α-$Co(OH)_2$ nanosheets water oxidation catalysts, J. Phys. Conf. Ser. (2016).
[30] N. Tiwari, S. Doke, A. Lohar, et al., J. Phys. Chem. Solids 90 (3) (2016) 100–113.
[31] H.B. Wang, Q. Wang, Y.D. Ji, et al., Mater. Sci. Forum 850 (2016) 5.
[32] S.A. Liu, Z.Z. Wang, S.G. Li, et al., Earth Planet. Sci. Lett. 444 (2016) 169–178.
[33] Y. Liu, Q.Q. Liu, X. Shen, X. Li, S.M. Feng, R.C. Yu, S. Uchida, C.Q. Jin, Physica C 497 (2014) 34–37.
[34] B. Ravel, M. Newville, J. Synchrotron Radiat. 12 (4) (2005) 537–541.
[35] Y. Joly, Phys. Rev. B 63 (12) (2001) 125120.